PROTEINS: Structure, Function, and Bioinformatics 67:243–246 (2007)

STRUCTURE NOTE

Crystal Structure of Chemically Synthesized vMIP-II

Ying Li,[1] Dongxiang Liu,[2] Rong Cao,[1] Santosh Kumar,[2] Changzhi Dong,[2] Jing An,[2,3] Scott R. Wilson,[4] Yi-Gui Gao,[4] and Ziwei Huang[1,2,4]*

[1]*Center for Biophysics and Computational Biology, University of Illinois at Urbana-Champaign, Urbana, Illinois 61801*
[2]*Department of Biochemistry, University of Illinois at Urbana-Champaign, Urbana, Illinois 61801*
[3]*Raylight Corporation, Chemokine Pharmaceutical Inc., La Jolla, California 92037*
[4]*Department of Chemistry, University of Illinois at Urbana-Champaign, Urbana, Illinois 61801*

Introduction. The viral inflammatory protein II (vMIP-II) is a mammalian chemokine homolog encoded by Kaposi's sarcoma-associated herpesvirus (KSHV).[1,2] Chemokines constitute the largest family of cytokines that play important roles in immune responses. The main biological function of chemokines is to mediate the recruitment of leukocytes to the site of inflammation and their activation.[3] The activity of chemokines is effected by binding to the G-protein coupled chemokine receptors present on various subpopulations of leukocytes such as monocytes, macrophages, basophils, eosinophils, and lymphocytes.[4]

Based on the positions of the first two conservative cysteine residues, chemokines are classified into four subfamilies: CXC, CC, CX3C, and C. As a viral chemokine, vMIP-II shows a broad spectrum of binding to CXC, CC, and CX3C chemokine receptors. In particular, vMIP-II binds to both CXCR4 and CCR5, which are the only two major coreceptors of human immunodeficiency virus Type 1 (HIV-1). Although most mammalian chemokines are agonists to their corresponding receptors, vMIP-II is in most cases an antagonist to its receptors including CXCR4 and CCR5.[2] All ligands of CXCR4 and CCR5 show anti-HIV activity *in vitro* by competing with HIV-1 for the binding of the coreceptors though some are more potent than others.[5]

The structural basis of the interaction between chemokines and their receptors was subjected to intense investigation in recent years. However, many of the details are still not known. Here, we report the crystal structure of vMIP-II in two crystal forms different from previously reported and discuss the structural features that are possibly related to the binding affinity and specificity.

Materials and Methods. vMIP-II was chemically synthesized in our lab according a previously published protocol.[6] The chemically synthesized vMIP-II was crystallized by hanging drop vapor diffusion using the condition reported by Fernandez et al.[7] Protein (10 mg/mL) was mixed at 1:1 ratio with reservoir solution, which is 100 m*M* sodium citrate buffer (PH = 5.6), 11% (w/v) PEG 4000, and 11% (w/v) 2-propanol.

The data sets were collected at the 19-BM beamline of the Advanced Photon Source at Argonne National Laboratory (Argonne, IL) and the X12C beamline of Light Source (LS) at Brookhaven National Laboratory (Upton, NY). The crystals were first soaked in cryoprotectant (35% sucrose) briefly and frozen in liquid nitrogen. The data was processed with HKL2000 software package.[8] The tetragonal crystal data set is 98.6% complete, consisting of 8305 unique reflections in the resolution range of 30–1.7 Å. The monoclinic crystal data set is 89.1% complete, consisting of 10,419 unique reflections in the resolution range of 30–2.3 Å. The crystal parameters and data collection conditions are summarized in Table I.

The crystal structure of vMIP-II was solved by molecular replacement using the program AmoRe.[9] For tetragonal crystal form, the A chain of the vMIP-II dimer (PDB code 1CM9) was used as the search model. The rigid body refinement was applied to the initial model. Then the structure was refined by simulated annealing using X-PLOR.[10] The missing sidechains of the initial model were added to the structure with the program O[11] whenever the corresponding electron density could clearly be seen in the $2F_o$–F_c map. Solvent molecules were finally added and verified by electron density map. During the process

Abbreviations: vMIP-II, viral macrophage inflammatory protein-II; MCP-2, monocyte chemoattractant protein-2; CXCR4, CXC chemokine receptor 4; CCR5, CC chemokine receptor 5; RMSD, root mean square deviations.

Grant sponsor: National Institutes of Health (NIH); Grant number: GM057761.

The coordinates of vMIP-II have been deposited into Protein Data Bank under accession code 2FHT and 2FJ2.

*Correspondence to: Z. Huang, The Burnham Institute for Medical Research, 10901 N. Torrey Pines Road, La Jolla, CA 92037.
E-mail: ziweihuang@burnham.org

Received 26 March 2006; Revised 30 June 2006; Accepted 9 July 2006

Published online 22 January 2007 in Wiley InterScience (www.interscience.wiley.com). DOI: 10.1002/prot.21172

TABLE I. Crystal Data and Experimental Details for vMIP-II Crystals

	Tetragonal	Monoclinic
Space group	$P4_1\,2\,2$	$P2_1$
Unit cell dimension	$a = b = 45.75$, $c = 66.36$	$a = 45.63$, $b = 65.77$, $c = 45.62$, $\beta = 91.62^\circ$
Molecules/asymmetric unit	1	4
Solvent content	38%	37%
X-ray source	19-BM, APS, ANL	X12C, BNL
Wavelength (Å)	0.9559	1.10
Resolution (Å)	1.7	2.3
Temperature (K)	100	100
Observed reflections	62,915	36,467
Unique reflections	8305	10,419
Overall completeness (%)	98.6	84.9
Overall R_{merge}[a]	0.058	0.051

[a] $R_{merge} = \Sigma|I_n - \langle I\rangle|/\Sigma\langle I\rangle$.

of further refinement, solvent molecules with *B*-factors higher than 70 were removed.

Results and Discussion. The vMIP-II structures in tetragonal and monoclinic crystal forms were determined to 1.7 and 2.3 Å, respectively, by molecular replacement method. Although the crystallization condition is the same as reported by Fernandez et al.,[7] we did not obtain the monoclinic crystals belonging to the same space group as previously reported.[7] Instead, we obtained both monoclinic crystals belonging to a different space group and tetragonal crystals. Similar phenomenon has been observed on the CC chemokine MCP-1.[12] In the previously reported monoclinic crystal, a noncrystallographic dimer was observed in the asymmetric unit, whereas our tetragonal crystal contains a monomer and our monoclinic crystal contains two dimers in the asymmetric unit. The overall monomer structure is shown in Figure 1(A). The structure refinement statistics is summarized in Table II. An example of electron density map is shown in Figure 1(B). The tertiary structure is consistent with many previously reported CC chemokine structures. The flexible N-terminus and N-loop are followed by three antiparallel β-strands (residues 25–30, 39–44, 49–53) arranged in a Greek key motif with a C-terminal α-helix (residues 57–65) laid on top of them. Interestingly, a water molecule buried inside the protein was observed in both crystal forms, which is hydrogen-bonded to the mainchain carbonyl of Lys37 and the sidechain hydroxyl group of Thr31. It is conservative in different crystals as it is also present in the previously reported crystal structure.[7] This water molecule may help to stabilize the conformation of the 30's loop between the first and the second β-strands. The RMSDs of Cα atoms between our structure and the previously reported crystal structure (PDB ID 1CM9) have been calculated. The RMSDs for chain A and chain B of the tetragonal crystal form are 0.56 and 0.52 Å, respectively. For the monoclinic crystal form, the RMSDs are 0.55, 0.42, 0.44, and 0.46 Å for A, B, C, and D chains, respectively.

By examining the molecules in neighboring asymmetric unit, it was found that vMIP-II forms crystallographic dimers in our tetragonal crystal through interactions between N-termini, which is the interaction pattern also observed in the asymmetric unit of previously reported crystal form. The dimer is stabilized by six pairs of H-bonds, among which the H-bond between sidechain carbonyl group of Gln16 and mainchain amide of Ser4 was not observed previously. There are also weak interactions between two dimers mainly through the contact of the N-terminus of one molecule with the C-terminus of a neighboring molecule. The C-terminal carboxyl group is hydrogen-bonded to the mainchain oxygen atom of Arg7 of the neighboring molecule. The interactions are also reflected on the relatively low *B*-factors of C-terminus, suggesting the stabilization of C-terminus by the neighboring molecule. The buried surface area is ~300 Å^2 for each dimer due to interactions on the dimer–dimer interface. Similar weak interactions are also observed in our monoclinic crystals but the relative orientation of two dimers is slightly different. In contrast, dimers do not interact with each other in the previously reported crystal structure. Therefore, vMIP-II seems to have a strong tendency to form dimers in a crystal environment but the interactions between dimers are weak and nonspecific.

One of the motivations to study chemokine structures is to understand the structural basis for chemokines to interact with their receptors. According to the two-site binding model,[14–16] the N-loop after the first pair of conservative cysteines participates in the initial ligand-receptor recognition. Among multiple mammalian chemokine ligands of CCR5, including MIP-1α, MIP-1β, RANTES, and MCP-2,[17,18] vMIP-II shares the highest sequence identity with MIP-1α and MIP-1β (52 and 47%, respectively). The sequence alignment of the five CCR5 ligands is shown in Figure 1(D). In the N-loop region, vMIP-II shares the most similar surface topology and electrostatic potential with RANTES among all the CCR5 ligands [Fig. 1(C)]. For these two ligands, the N-loop and surrounding regions are, to a large extent, positively charged, while MIP-1α and MIP-1β are almost apolar in the corresponding regions. Arg18 is one of the conserved residues in the N-loop region. The importance of this Arg18 was confirmed in MIP-1β by mutagenesis studies.[19] However, it is not necessarily essential for all the ligands with RANTES as an example.[20] For MIP-1α and MIP-1β, the sidechain of this Arg18 protrudes far

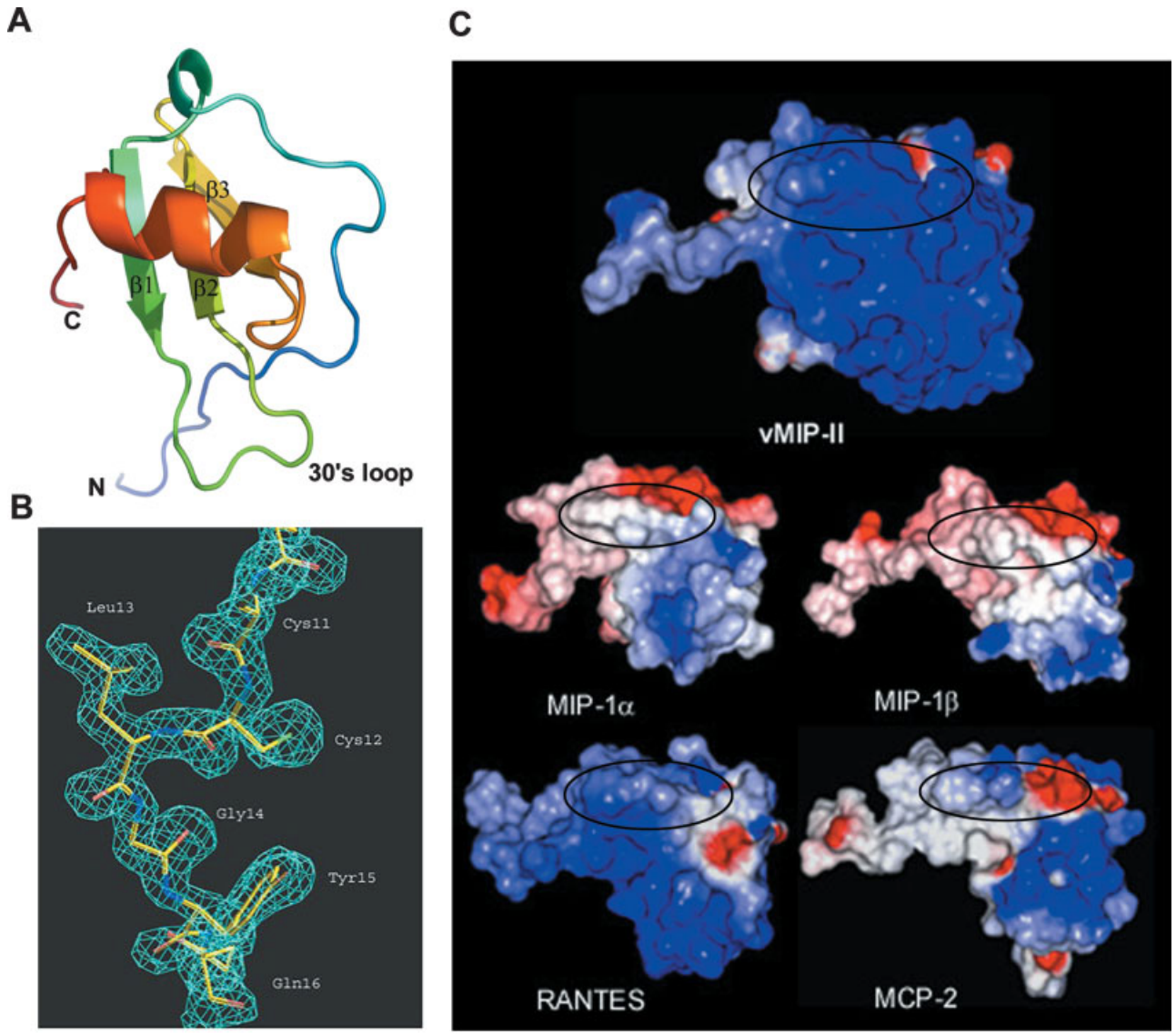

D

```
vMIP-II LGASWHRPDKCCLGYQKRPLPQVLLSSWYPTSQL-CSKPGVIFLTKRGRQVCADKSKDWVKKLMQQLPVTAR---
MIP-1α  -SLAADTPTACCFSYTSRQIPQNFIADYFETSSQ-CSKPGVIFLTKRSRQVCADPSEEWVQKYVSDLELSA----
MIP-1β  APMGSDPPTACCFSYTARKLPRNFVVDYYETSSL-CSQPAVVFQTKRSKQVCADPSESWVQEYVYDLELN-----
RANTES  -PYSSDT-TPCCFAYIARPLPRAHIKEYFYTSGK-CSNPAVVFVTRKNRQVCANPEKKWVREYINSLEMS-----
MCP-2   MPDSVSIPITCCFNVINRKIPIQRLESYTRITNIQCPKEAVIFKTQRGKEVCADPKERWVRDSMKHLDQIFQNLK
```

Fig. 1. (A) The structural diagram of vMIP-II monomer containing residues 4–71 (tetragonal crystal form). (B) The residues 11–16 of vMIP-II monomer in tetragonal crystal form with $2F_o–F_c$ electron density map contoured at 1.0σ. The figure was produced by program O.[11] (C) The solvent accessible surface of vMIP-II (this work), MIP-1α (PDB code 1B53), MIP-1β (PDB code 1HUM), RANTES (PDB code 1B3A), and MCP-2 (PDB code 1ESR).The surfaces are colored according to surface electrostatic potential calculated by DelPhi.[13] Red color represents negative electrical potential and blue color represents positive electrical potential. The N-loop regions of each structure were circled. (D) Sequence alignment of vMIP-II, MIP-1α, MIP-1β, RANTES, and MCP-2. The N-loop loop region is represented in bold letters.

out of the protein surface, whereas in all other ligands it assumes a conformation bending toward the surface. The extended sidechain conformations in MIP-1α and MIP-1β possibly facilitate the charge–charge interaction between ligands and receptors considering the aforementioned fact that the N-loop regions are relatively apolar for these two CCR5 ligands. Overall, the structural comparison of the N-loop region suggests that high sequence identity and the presence of conserved residues do not necessary lead to similar local geometry and electrostatic potential in the functional sites, which is probably one of the reasons why the structure scaffolds

TABLE II. Structure Refinement Statistics of vMIP-II Crystals

	Tetragonal	Monoclinic
Resolution range (Å)	6.0–1.7	10–2.3
Final *R*-factor[a]/free *R*-factor (7%)	0.242/0.333	0.246/0.303
Number of residues/refined non-H atoms	71/531	284/2088
Number of solvent molecules	27	99
Average *B*-factor		
Mainchain	28.32	34.52
Sidechain	34.66	35.42
Overall	31.42	34.95
Solvent	43.86	43.37
RMSD for ideality in		
Bond length (Å)	0.010	0.015
Bond angle (°)	1.589	1.539

[a] $F > 4\sigma(F)$ data.

of all chemokines are very similar but the binding specificity and affinity are distinct.

Acknowledgments. We thank Dr. Randy Alkire at SBC 19-BM beamline, Argonne National Laboratory, for his help on the data collection and Dr. Howard Robinson at Brookhaven National Laboratory for collecting the monoclinic crystal data set. The use of the Argonne National Laboratory Structural Biology Center beamlines at the Advanced Photon Source is supported by the U. S. Department of Energy, Office of Energy Research, under Contract No. W-31-109-ENG-38.

REFERENCES

1. Russo JJ, Bohenzky RA, Chien MC, Chen J, Yan M, Maddalena D, Parry JP, Peruzzi D, Edelman IS, Chang Y, Moore PS. Nucleotide sequence of the Kaposi sarcoma-associated herpesvirus (HHV8). Proc Natl Acad Sci USA 1996;93:14862–14867.
2. Kledal TN, Rosenkilde MM, Coulin F, Simmons G, Johnsen AH, Alouani S, Power CA, Luttichau HR, Gerstoft J, Clapham PR, Clark-Lewis I, Wells TN, Schwartz TW. A broad-spectrum chemokine antagonist encoded by Kaposi's sarcoma-associated herpesvirus. Science 1997;277:1656–1659.
3. Baggiolini M, Dewald B, Moser B. Human chemokines: an update. Annu Rev Immunol 1997;15:675–705.
4. Horuk R. Chemokine receptors. Cytokine Growth Factor Rev 2001;12:313–335.
5. Baldwin ET, Weber IT, St Charles R, Xuan JC, Appella E, Yamada M, Matsushima K, Edwards BF, Clore GM, Gronenborn AM, Wlodawer A. Crystal structure of interleukin 8: symbiosis of NMR and crystallography. Proc Natl Acad Sci USA 1991;88:502–506.
6. Kumar S, Choi WT, Madani N, Dong CZ, Tian S, Liu D, Fan X, Wang Y, Pesavento J, An J, Sodroski JG, Hunag Z. SMM-chemokines: a new class of unnatural synthetic molecules as chemical probes of chemokine receptor biology and lead for therapeutic development. Chem Biol 2006;13:69–79.
7. Fernandez EJ, Wilken J, Thompson DA, Peiper SC, Lolis E. Comparison of the structure of vMIP-II with eotaxin-1, RANTES, and MCP-3 suggests a unique mechanism for CCR3 activation. Biochemistry 2000;39:12837–12844.
8. Otwinowski Z, Minor W. Processing of X-ray diffraction data collected in oscillation mode. Methods Enzymol 1997;276:307–326.
9. Navaza J. Amore—an Automated Package for Molecular Replacement. Acta Crystallogr Sect A 1994;50:157–163.
10. Brunger AT. X-PLOR Version 3.1: a system for X-ray crystallography and NMR. New Haven: Yale University Press; 1992.
11. Jones TA, Zou JY, Cowan SW, Kjeldgaard M. Improved methods for building protein models in electron-density maps and the location of errors in these models. Acta Crystallogr Sect A 1991; 47:110–119.
12. Lubkowski J, Bujacz G, Boque L, Domaille PJ, Handel TM, Wlodawer A. The structure of MCP-1 in two crystal forms provides a rare example of variable quaternary interactions. Nat Struct Biol 1997;4:64–69.
13. Honig B, Nicholls A. Classical electrostatics in biology and chemistry. Science 1995;268:1144–1149.
14. Crump MP, Gong JH, Loetscher P, Rajarathnam K, Amara A, Arenzana-Seisdedos F, Virelizier JL, Baggiolini M, Sykes BD, Clark-Lewis I. Solution structure and basis for functional activity of stromal cell-derived factor-1; dissociation of CXCR4 activation from binding and inhibition of HIV-1. EMBO J 1997;16:6996–7007.
15. Lowman HB, Slagle PH, DeForge LE, Wirth CM, Gillece-Castro BL, Bourell JH, Fairbrother WJ. Exchanging interleukin-8 and melanoma growth-stimulating activity receptor binding specificities. J Biol Chem 1996;271:14344–14352.
16. Monteclaro FS, Charo IF. The amino-terminal extracellular domain of the MCP-1 receptor, but not the RANTES/MIP-1alpha receptor, confers chemokine selectivity. Evidence for a two-step mechanism for MCP-1 receptor activation. J Biol Chem 1996;271: 19084–19092.
17. Wells TN, Power CA, Lusti-Narasimhan M, Hoogewerf AJ, Cooke RM, Chung CW, Peitsch MC, Proudfoot AE. Selectivity and antagonism of chemokine receptors. J Leukoc Biol 1996;59:53–60.
18. Gong W, Howard OM, Turpin JA, Grimm MC, Ueda H, Gray PW, Raport CJ, Oppenheim JJ, Wang JM. Monocyte chemotactic protein-2 activates CCR5 and blocks CD4/CCR5-mediated HIV-1 entry/replication. J Biol Chem 1998;273:4289–4292.
19. Bondue A, Jao SC, Blanpain C, Parmentier M, LiWang PJ. Characterization of the role of the N-loop of MIP-1β in CCR5 binding. Biochemistry 2002;41:13548–13555.
20. Pakianathan DR, Kuta EG, Artis DR, Skelton NJ, Hebert CA. Distinct but overlapping epitopes for the interaction of a CC-chemokine with CCR1, CCR3 and CCR5. Biochemistry 1997;36: 9642–9648.